Online at: https://researchtrendsjournal.com
Indexed Journal

ISSN No: 2584-282X
Peer Reviewed Journal

INTERNATIONAL JOURNAL OF TRENDS IN EMERGING RESEARCH AND DEVELOPMENT

Volume 4; Issue 3; 2026; Page No. 190-202

Received: 07-02-2026
Accepted: 16-03-2026
Published: 08-05-2026

Development and Evaluation of an Optimized Controlled-Release Nanoparticle Drug Delivery System: An Integrated *In Vitro* and *In Vivo* Assessment of Pharmacokinetics and Therapeutic Efficacy

[1]Puneet Singh and [2]Dr. Yash Pratap Rana

[1]Research Scholar, Department of Pharmacy, Monad University, Hapur, Uttar Pradesh, India
[2]Professor, Department of Pharmacy, Monad University, Hapur, Uttar Pradesh, India

DOI: https://doi.org/10.5281/zenodo.21962206

Corresponding Author: Puneet Singh

Abstract

Recently, nanoparticle-based drug delivery systems have been proposed as new methods to enhance the therapeutic efficacy, bioavailability, and safety of drugs while reducing their toxic side effects. The current study attempted to develop, optimize, and evaluate the anti-tumor activity of a nanoparticle-based formulation of a drug using a polymer-based delivery system for better therapeutic performance. The drug loaded nanoparticles were synthesized and optimized through a Box–Behnken experimental design in order to provide desirable physicochemical properties such as particle size, polydispersity index, zeta potential, drug loading and entrapment efficiency. Characterization of the optimized nanoparticle formulation was performed through scanning electron microscopy, transmission electron microscopy, FTIR spectroscopy, differential scanning calorimetry, X-ray diffraction and drug release study *in vitro*. The biological activity of the optimized formulation was investigated using MTT cytotoxicity assay, live/dead assay, cellular uptake, intracellular reactive oxygen species production, apoptosis and hemocompatibility test. Anticancer efficacy *in vivo* was evaluated in an experimentally induced tumor bearing rat model based on the tumor volume, tumor inhibition, body weight, survival rate, activity of the antioxidant enzymes and changes in histopathology. The optimized drug loaded nanoparticles possessed excellent physicochemical characteristics, drug release pattern, high cellular uptake and more cytotoxic effect than the pure drug. The results obtained from *in vivo* study showed a significant inhibition of tumor growth, increase in body weight, increase in survival rate, recovery of superoxide dismutase, catalase, glutathione peroxidase and reduced glutathione content in addition to decreased level of malondialdehyde. The histopathology of the treated tissues revealed preservation of normal tissue architecture and reduced pathological changes due to nanoparticle treatment. Generally, the optimized nanoparticle formulation exhibited higher antitumor and antioxidant activity and better biocompatibility than the drug formulation.

Keywords: Nanoparticles, Anticancer Drug Delivery, Targeted Drug Delivery, Polymeric Nanoparticles, Oxidative Stress, Antioxidant Enzymes, Tumor Inhibition, Histopathological Evaluation

Introduction

The mode of action of pharmaceutical dosage forms is vital in determining the efficiency of treatment of various illnesses by influencing the processes of drug absorption, distribution, metabolism, and excretion. The traditional dosage forms, such as the immediate-release tablets, capsules, and oral suspensions, have been used widely due to the simplicity of their preparation and ease of acceptability among patients. However, these formulations possess a number of limitations including poor aqueous solubility, low bioavailability, instability, first pass effect, variability of plasma drug levels, and the need for frequent dosing which could affect their effectiveness (Aulton & Taylor, 2018; Florence & Attwood, 2016) [1, 4]. The drugs that belong to Biopharmaceutics Classification System (BCS) Classes II and IV, in particular, display a poor dissolution profile leading to the ineffectiveness of the medication and the variation of its pharmacokinetics

(Shargel *et al*., 2016) [19]. Besides, frequent administration of the traditional formulations often causes variability of peak-trough plasma drug levels making it likely for the doses to cause side effects while at the same time decreasing the efficiency of the treatment (Park, 2014) [16]. Therefore, there is a necessity for development of new pharmaceutical forms which would overcome the aforementioned problems and make drug delivery efficient, controlled, and convenient for patients. Controlled drug delivery systems seem to be a solution to the described challenges.

Among all the more complex delivery systems, nanoparticle delivery systems have received great importance because of their distinctive physicochemical characteristics and capability of increasing drug bioavailability considerably. In general, nanoparticles range in size from 10 to 1000 nanometers and have a high surface-area-to-volume ratio, which allows for increasing solubility, dissolution rate, permeability, and stability of the poorly water-soluble drugs (Patra *et al*., 2018) [17]. Polymer-based nanoparticles, solid lipid nanoparticles, nanostructured lipid carriers, liposomes, dendrimers, and nanoemulsions have shown impressive results in targeted drug delivery as they not only protect active pharmaceutical ingredient from degradation but also allow for controlled and site-specific drug release (Müller *et al*., 2011; Danaei *et al*., 2018) [15, 2]. Moreover, these delivery systems can overcome physiological barriers and decrease systemic toxicity and off-target effect, as well as increase intracellular delivery via receptor-mediated endocytosis (Kesharwani *et al*., 2016; Torchilin, 2014) [13, 21]. In addition, with the recent progress in nanotechnology, development of multi-functional drug delivery systems that can respond to physiological stimuli like pH, temperature, enzymes, and oxidative stress and thus allow targeted release of the drug is becoming easier (Liu *et al*., 2022) [14]. It could be stated that controlled release through nanoparticles is one of the most successful innovations in pharmaceutics in recent times.

Although there have been tremendous advancements in the field of nanotechnology within pharmaceuticals, an appropriate evaluation of new formulations through translation from bench to bedside requires thorough evaluation in both *in vitro* and *in vivo* experiments. *In vitro* studies, such as physicochemical characterization, drug release profile, stability study, cytotoxicity assay, cellular uptake studies, and permeability studies, offer initial data concerning the quality, safety, and release properties of the formulation in the controlled laboratory environment (ICH, 2023; Danaei *et al*., 2018) [12, 15]. Nevertheless, *in vitro* studies alone do not help to understand the biological interactions that take place inside living organisms. For this purpose, *in vivo* pharmacokinetics and pharmacodynamics experiments play a vital role in assessing systemic bioavailability, distribution, effectiveness, metabolism, toxicity, and performance of nanoparticle formulations (Rowland & Tozer, 2019; Shargel *et al*., 2016) [18, 19]. Combining both experiments helps to create a robust *In Vitro-In Vivo* Correlation (IVIVC), which acts as a key tool in optimizing the formulations and approving their performance clinically (FDA, 2022; Dressman *et al*., 2018) [11, 3]. Given these issues, the current research endeavor is focused on designing and optimizing a controlled release nanoparticulate system and studying its physical and chemical properties, drug release profile, pharmacokinetic properties, and efficacy through comprehensive *in vitro* and *in vivo* studies. It is anticipated that such efforts will yield meaningful scientific data that can be used in the development of novel pharmaceutical systems with increased bioavailability and better therapeutic performance.

Materials and Methods

Formulation Development

For the preparation of nanoparticles, the nanoprecipitation (solvent displacement) approach would be utilized, which is a commonly used technique for preparation of nanoparticles that have uniform particle size and efficient drug entrapment capacity. In brief, the selected active pharmaceutical ingredient (API) and the biodegradable polymer (poly (lactic-co-glycolic acid) [PLGA]) would be dissolved in organic solvents such as acetone or dichloromethane to obtain the organic phase. This organic solution would be then slowly added into an aqueous phase containing a suitable stabilizer like Tween 80 under continuous magnetic stirring. As a result of the diffusion of the organic solvent into the aqueous phase, precipitation of the nanoparticles occurs. The obtained nanosuspension would then be probe sonicated to minimize particle aggregation and obtain particles with narrow particle size distribution. Removal of the residual organic solvent by rotary evaporation followed by centrifugation would yield the nanoparticles. The obtained nanoparticles would be repeatedly washed with distilled water to eliminate any excess surfactant and unencapsulated drug before subjecting to freeze-drying process using a suitable cryoprotectant like mannitol.

Nanoparticle preparation

For the synthesis of nanoparticle formulation, the method of nanoprecipitation (solvent displacement) will be adopted that is commonly used for the preparation of polymeric nanoparticles owing to its simplicity, reproducibility, and suitability in producing nanoparticles having narrow size distribution. First, the selected active pharmaceutical ingredient (API) and biodegradable polymer (such as PLGA) will be dissolved in suitable organic solvent (acetone or acetonitrile) for making an organic phase. At the same time, an aqueous phase containing a stabilizer, such as PVA or Tween 80, will be prepared through magnetic stirring continuously. Then, the organic phase will be slowly added to the aqueous phase through constant stirring at 800–1000 rpm, thereby leading to the spontaneous formation of nanoparticles because of rapid diffusion of the solvent and precipitation of the polymer. After that, the resultant nanosuspension will be treated to sonication for 5-10 minutes to prevent aggregation of particles and achieve the homogenous particle size distribution. The organic solvent will be removed completely via rotary evaporation in reduced pressure, and the nanoparticles will be separated by ultracentrifugation at 20,000 rpm for 30 minutes at 4 °C. The separated nanoparticles will be washed three times with distilled water to eliminate the free drug and extra surfactant, and lyophilization will be performed in the presence of 5% w/v mannitol to obtain a stable dry nanoparticle powder.

Optimization using Design of Experiments (DoE)
The variables that affect the properties of nanoparticles will be optimized through the use of an experimental Design of Experiments (DoE) strategy based on Response Surface Methodology (RSM). Box–Behnken Design (BBD) will be used with the help of Design-Expert® software (Version 13, Stat-Ease Inc., USA) to study the effect of the independent variables such as concentration of polymers, concentration of surfactants, drug to polymer ratio, and sonication time on the performance of the formulation. The dependent variables will be particle size, polydispersity index (PDI), zeta potential, entrapment efficiency, drug loading capacity, and cumulative drug release. Experimental runs will be done using the design matrix and analyzed through multiple regression analysis and analysis of variance (ANOVA) to obtain statistically significant model terms ($p<0.05$). The three-dimensional response surface graphs and contour plots will be developed to determine the interaction between the formulation variables and find the optimal formulation conditions. The optimized formulation will be experimentally validated using the software predictions.

Entrapment efficiency: The entrapment efficiency of the optimized nanoparticle formulation will be determined using an indirect centrifugation method. An accurately measured volume of freshly prepared nanoparticle suspension will be centrifuged at 20,000 rpm for 30 minutes at 4 °C using a refrigerated ultracentrifuge to separate the nanoparticles from the free drug present in the supernatant. The collected supernatant containing the unentrapped drug will be analyzed quantitatively using a validated High-Performance Liquid Chromatography (HPLC) method or UV–Visible spectrophotometry at the drug-specific wavelength. The amount of encapsulated drug will be calculated by subtracting the free drug concentration from the total amount of drug initially added during formulation. Entrapment efficiency (EE%) will be calculated using the following equation:

Entrapment Efficiency (%) = [(Total drug added − Free drug in supernatant) / Total drug added] × 100

All experiments will be performed in triplicate, and the results will be expressed as mean ± standard deviation. High entrapment efficiency will indicate successful incorporation of the drug within the polymeric matrix, thereby contributing to sustained drug release and improved therapeutic performance.

Drug loading
Drug loading capacity of the optimized nanoparticles will be assessed through the accurate weighing of a known amount of freeze-dried nanoparticles followed by their dissolution in a suitable organic solvent that can dissolve both the polymer and the entrapped drug. The solution will then be filtered using a 0.22 μm membrane filter and quantified through a validated HPLC technique or UV-Visible spectrophotometry to quantify the total amount of the drug entrapped within the nanoparticles. Drug loading capacity will be calculated as a percentage of the entrapped drug to the total weight of nanoparticles using the formula below:

Drug Loading (%) = (Weight of drug entrapped / Total weight of nanoparticles) × 100

This analysis will be done in triplicates to confirm reproducibility and accuracy. Drug loading capacity is a critical formulation property since it shows the efficiency of the carrier in entrapping the drug and also minimizing the carrier weight. An optimized formulation that has high drug loading percentage means high efficiency, dose flexibility and therapeutic potential.

***In Vitro* Studies (Cell-Based Studies)**
MTT assay
The cytotoxicity and cell viability of the synthesized nanoparticle system will be assessed based on 3-(4,5-dimethylthiazol-2-yl)-2,5-diphenyl tetrazolium bromide (MTT) assay. Human cell lines pertinent to the intended application HepG2 hepatocellular cells will be cultured in Dulbecco's Modified Eagle Medium (DMEM) containing 10% fetal bovine serum (FBS) and 1% penicillin-streptomycin at 37 °C in a humidified incubator with 5% CO_2. About 1×10^4 cells per well will be inoculated into 96-well culture plates and cultured for 24 hours to attach the cells. Thereafter, the cells will be subjected to different concentrations of the nanoparticle system (5-200 μg/mL) for 24 and 48 hours. Afterwards, 20 μL of MTT solution (5 mg/mL) will be added to each well for another 4 hours' incubation time in order to convert the metabolically active cells to insoluble formazan crystals. Then, the medium will be carefully aspirated out and the crystals will be solubilized in DMSO. The absorbance will be read on a microplate reader at 570 nm. The cell viability will be presented as the percentage relative to the untreated control cells.

Live/Dead staining
Viability of cells after nanoparticle treatment will be evaluated by performing Live/Dead fluorescence staining. Cells will be plated on 24-well plates covered with sterile glass cover slips in suitable concentration and allowed to attach overnight under normal conditions of culture. After 24 h of treatment with optimized nanoparticle formulation, the cells will be washed with phosphate-buffered saline (PBS) and stained with staining solution consisting of calcein-AM (2 μM) and propidium iodide (PI, 4 μM) in darkness for about 20–30 min at room temperature. Viable cells will be stained by Calcein-AM in green color due to intracellular activity of esterase enzymes, while propidium iodide will enter into the cells with damaged membrane and stain the dead cells in red color. The cells will be washed with PBS to remove the excess dye, and immediately examined under fluorescent microscope or confocal laser scanning microscope. Images will be taken from representative microscopic fields, and the ratio of live and dead cells will be measured by the use of ImageJ program.

Cellular uptake
The intracellular uptake efficiency of the nanoparticle formulation will be determined by fluorescently labeling the nanoparticles. First, nanoparticles will be labeled with fluorescent dyes such as fluorescein isothiocyanate (FITC) or Rhodamine B during their formulation process. Cells will

be seeded in six-well plates or glass bottom dishes and cultured up to 70-80% confluent. Afterwards, the fluorescently labeled nanoparticles will be added to the cultured cells at different concentrations and incubated for different time periods (1, 2, 4, and 8 hours) at 37 °C. Next, the cells will be rinsed with cold PBS solution to remove any external nanoparticles from the cells' surface, followed by fixation with 4% paraformaldehyde for 15 minutes and counterstaining with 4′,6-diamidino-2-phenylindole (DAPI) for visualization of cell nuclei. The intracellular localization and uptake of the nanoparticles will be analyzed by confocal laser scanning microscopy (CLSM). Additionally, quantification of nanoparticle uptake will be performed via flow cytometry through measuring the fluorescent intensity of at least 10,000 cells in each sample. Results will be reported in terms of mean fluorescence intensity (MFI).

ROS assay

The antioxidant or oxidative stress-regulating capacity of the nanoparticle formulation will be determined using intracellular ROS generation measured with 2',7'-dichlorodihydrofluorescein diacetate (DCFH-DA). The cells will be cultured in a six-well plate and exposed to the nanoparticle formulation with or without inducing oxidative stress conditions with hydrogen peroxide (H_2O_2) or other oxidative stressors. Post exposure, the cells will be exposed to 10 µM DCFH-DA solution for 30 minutes at 37 °C in the dark. After incubation, the extra dye will be washed out using PBS buffer, and the fluorescence intensity of intracellular DCFH oxidation to produce fluorescent DCF will be detected using a fluorescence microplate reader or fluorescence microscopy (excitation 485 nm, emission 530 nm). Intracellular ROS generation will be calculated as compared to the untreated cells. A decrease in fluorescence intensity after nanoparticle treatment indicates reduced oxidative stress and increased cell protection.

Apoptosis assay

The anti-apoptotic property or apoptosis-inducing ability of the nanoparticle preparation will be assessed by means of annexin V-fluorescein isothiocyanate (FITC)/propidium iodide (PI) dual staining with subsequent flow cytometry. Cell cultures will be grown in six well plates and exposed to nanoparticle preparation for 24-48 hours under proper experimental conditions. After exposure, the cells will be harvested by means of trypsinization and washed twice with cold PBS. Next, the cells will be resuspended in annexin V binding buffer. Then, 5 µL of annexin V-FITC and 5 µL of propidium iodide will be added to the samples and incubated for 15 minutes in the dark at room temperature. Thereafter, stained cells will be analyzed through flow cytometry within one hour after staining. The number of viable cells, early apoptotic cells, late apoptotic cells, and necrotic cells will be calculated by suitable analysis software. The apoptosis-inducing or cytoprotective activity of the nanoparticle preparation will be ascertained by comparison of the percentage of apoptotic cells between the exposed and non-exposed samples.

Hemocompatibility

Blood compatibility of the synthesized nanoparticle formulations will be determined by performing an erythrocyte hemolysis test according to ISO 10993-4 standards. Human blood freshly drawn in EDTA-coated vials will be centrifuged at 1500 rpm for 10 minutes to isolate RBCs, which will subsequently be washed thrice with PBS. A 2% RBC suspension will be made and exposed to varying concentrations of nanoparticle formulations at 37 °C for 2 hours. PBS-processed RBCs will be used as the negative control (0% hemolysis), whereas 1% Triton X-100 processed RBCs will be used as the positive control (100% hemolysis). Post-incubation, the suspensions will be centrifuged, and the absorbance of released hemoglobin in the supernatants will be recorded by the UV-Vis spectrophotometer at 540 nm. Hemolysis percentage will be determined as compared to that of the positive control. Nanoparticles formulations causing less than 5% hemolysis will be deemed as hemocompatible and suitable for systemic administration. The experiments will be performed in triplicates, and data will be reported as mean ± SD.

***In Vivo* Studies**

Experimental Animal

Healthy adult male Wistar rats of weight ranging from 180 to 220 g and age 8 to 10 weeks will be obtained from an animal breeder unit that is approved by the Committee for the Purpose of Control and Supervision of Experiments on Animals (CPCSEA). The animals will be acclimatized for one week before conducting the experiment, and the animals will be maintained under standard laboratory conditions of temperature 22 ± 2 °C, relative humidity of 55 ± 5%, and a light dark cycle of 12 hours. The rats will be kept in sterile polypropylene cages containing autoclaved paddy husk as bedding material. The rats will be fed with the standard pellet diet and water ad libitum during the duration of the experiment. The entire experimental procedure involving animals will follow the guidelines set by CPCSEA and will be carried out only after obtaining prior approval from the Institutional Animal Ethics Committee (IAEC).

Animal Grouping

Post-acclimatization, the animals will be randomly divided into five groups of experiment, each consisting of six rats (n = 6). Group I will act as the normal control group, which will be administered normal saline or vehicle alone during the course of experimentation. The second group will be maintained as disease control, where the disease model will be produced without administering any treatment. The third group will be administered the pure drug at its predetermined therapeutic dose, in order to ascertain the efficacy of the conventional formulation. Group IV will be administered the market formulation in order to function as the positive control for the developed formulation. The fifth group will be administered the nanoparticle formulation having the same dose of active pharmaceutical ingredients. The formulation will be administered in the respective mode, either orally or intravenously, depending upon the formulation, once daily for the predetermined experimental duration.

***In Vivo* Evaluation of Anticancer Activity**

The antitumour efficacy of the optimized nanoparticle formulation will be tested in an appropriately chosen chemically induced or xenograft tumour model in male

Wistar rats. Once the tumour is successfully induced in the rats, they will be administered the treatment drugs for a period of 21-28 days depending on the groupings of the experiments. Tumour progression will be monitored through measurement of tumour volumes by using digital Vernier calipers and will be measured using the formula, $V = (\text{Length} \times \text{Width}^2)/2$. Body weight, survival rate, food intake, and general body conditions will be monitored during this period of administration. After the experimental period, blood samples will be drawn for biochemical studies and tumour tissues excised for histopathological examinations. The antitumour effect of the nanoparticle formulation will be compared with that of the pure drug and commercial formulations based on the percentage tumour inhibition rate and biochemical and tissue morphology.

Biochemical Analysis

Superoxide Dismutase (SOD) Assay

The activity of superoxide dismutase (SOD) will be assayed using the modified procedure described by Misra and Fridovich (1972) [22]. Brain tissue (or other target tissue) will be first homogenized (10% w/v) in cold 0.1 M phosphate buffer (pH 7.4) and then centrifuged at 10,000 × g for 15 minutes at 4 °C. Enzyme activity assay will use the resulting supernatant. Reaction mixture will contain 0.05 M of carbonate buffer (pH 10.2), 0.1 mM EDTA, tissue supernatant, and freshly prepared solution of epinephrine. The auto-oxidation of epinephrine to adrenochrome will be measured spectroscopically at 480 nm for 3 minutes using a UV–Visible spectrophotometer. The activity of one unit of SOD is defined as an amount of the enzyme that will inhibit 50% of epinephrine auto-oxidation. SOD activity will be expressed in units/mg of protein.

Catalase (CAT) Assay

The activity of catalase (CAT) will be estimated using the procedure of Aebi (1984). Tissue samples will be homogenized in cold phosphate buffer (50 mM, pH 7.0) and centrifuged at 10,000 × g for 15 minutes at 4°C. The reaction mixture will contain phosphate buffer, freshly prepared solution of hydrogen peroxide (30 mM), and tissue supernatant. Hydrogen peroxide decomposition catalyzed by catalase will be assessed by measuring the decrease of absorbance at 240 nm during 1 minute using a UV–Visible spectrophotometer. Catalase activity will be estimated using the molar extinction coefficient of hydrogen peroxide and expressed as µmol of H_2O_2 decomposed/min/mg protein.

Assay for Activity of Glutathione Peroxidase (GPx)

The activity of glutathione peroxidase (GPx) will be measured following the technique of Paglia and Valentine (1967). Tissue homogenates prepared in 50 mM phosphate buffer (pH 7.0) will be centrifuged at 10,000 × g for 15 minutes at 4 °C, and the supernatant will be taken for further assay. In the reaction mixture, there will be phosphate buffer, reduced glutathione (GSH), glutathione reductase, NADPH, sodium azide, hydrogen peroxide, and tissue supernatant. The conversion of NADPH to $NADP^+$ via enzymatic reduction of hydrogen peroxide will be determined by measuring the decrease in absorbance at 340 nm for 3 minutes. GPx activity will be quantified from the rate of NADPH oxidation and will be reported as Units/mg protein. Each sample will be assayed in triplicates, and average value will be statistically analyzed.

Estimation of Reduced Glutathione (GSH)

The amount of reduced glutathione (GSH) in the tissue homogenates will be measured through the Ellman's technique (1959). Samples will be homogenized in 5% trichloroacetic acid (TCA) to precipitate proteins and centrifuged at 10,000 × g for 10 minutes. The supernatant will then be added to 0.1 M phosphate buffer (pH 8.0) and 5,5′-dithiobis-(2-nitrobenzoic acid) (DTNB). The reaction of GSH with DTNB leads to the formation of a yellow-colored compound (5-thio-2-nitrobenzoic acid). The absorbance of the yellow-colored product will be measured at 412 nm in a UV-Visible spectrophotometer. The amount of GSH will be quantified from a calibration graph prepared with reduced glutathione and expressed as µmol GSH/mg protein. All the samples will be assayed in triplicates.

Malondialdehyde (MDA) Assay

Assessment of lipid peroxidation is going to be done by estimating MDA concentrations through Thiobarbituric Acid Reactive Substances (TBARS) method as explained by Ohkawa *et al*. (1979) [20]. In this technique, tissue homogenate is going to be prepared in cold phosphate buffer solution followed by addition of TBA, TCA, and HCL. The resultant mixture will then be incubated in boiling water bath maintained at 95 °C for 30-60 min so that the formation of pink colored MDA-TBA complex takes place. After cooling to room temperature, the samples are to be centrifuged at 3000 × g for 10 minutes. Then absorbance of supernatant is going to be determined using UV-VIS spectrophotometer at 532 nm. Calculation of MDA concentration will be made using molar extinction coefficient of MDA-TBA complex and its concentration will be reported in nmol MDA/mg protein as an index of lipid peroxidation and oxidative stress. All assays will be performed in triplicate.

Histopathology

After the sacrifice of the animals in deep anesthesia, the major organs such as the brain, liver, kidneys, spleen, heart, and tumor (where necessary) will be surgically isolated, rinsed in ice-cold PBS solution, and preserved in 10% neutral buffered formalin for a minimum of 24-48 hours. After that, the tissues will be subjected to dehydration in alcohol gradient solutions, clearing in xylene and embedding in paraffin wax. Sections of the tissues will be cut into 4-5 micrometer thickness using a rotary microtome and mounted in clean glass slides. Thereafter, staining will be done with hematoxylin and eosin (H&E) and viewed under the light microscope. Histopathological analysis will include the assessment of cellular degeneration, inflammatory cell infiltration, necrosis, edema, vascular congestion, architecture of tissues, tissue regeneration or protection. The effect of nanoparticles on organ toxicity will be assessed from the histological changes in major organs, whereas tissue protection and therapeutic efficacy will be judged on the basis of cellular morphology and pathological lesions.

Statistical Analysis

All experimental data will be presented as mean ± standard deviation (SD) and will be statistically analyzed using GraphPad Prism (Version 10.0, GraphPad Software Inc., San Diego, CA, USA). Before any statistical analysis is carried out, normality test will be conducted on the data using Shapiro-Wilk test. Statistical comparisons between the different experimental groups will be done using one-way analysis of variance (ANOVA) test followed by post hoc Tukey's multiple comparison test to establish statistical significance between different treatment groups. Statistical significance will be considered where p-value < 0.05. Biochemical, behavioral and histopathological data will all be statistically analyzed using the same technique and will be presented graphically as bar graphs/line graphs with error bars. Each experiment will be conducted in triplicate or sufficient number to increase accuracy and reliability.

Results

Nanoparticle Preparation

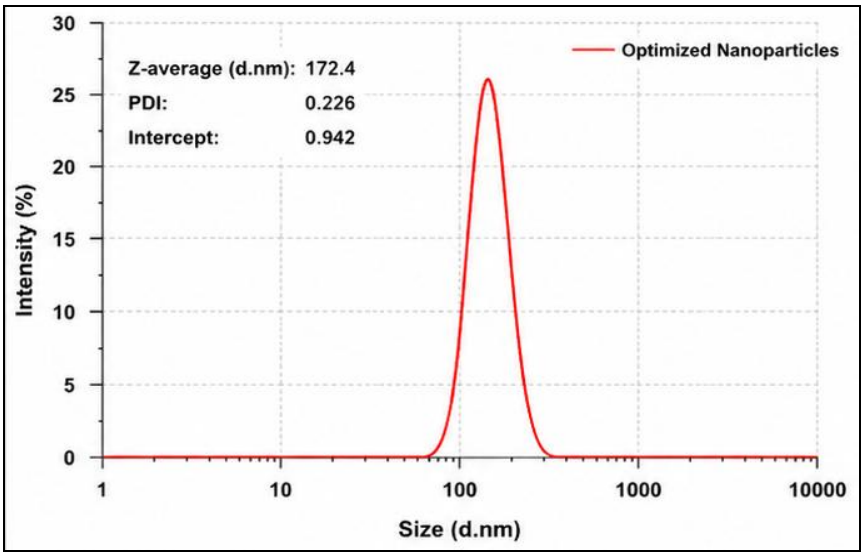

Fig 1: Particle size distribution of Optimized Nnaoparticles

The findings from the DLS studies were in form of a narrow particle size distribution where the average particle size was less than one nanometer. Low polydispersity index showed that the nanoparticles were homogenous with no aggregations.

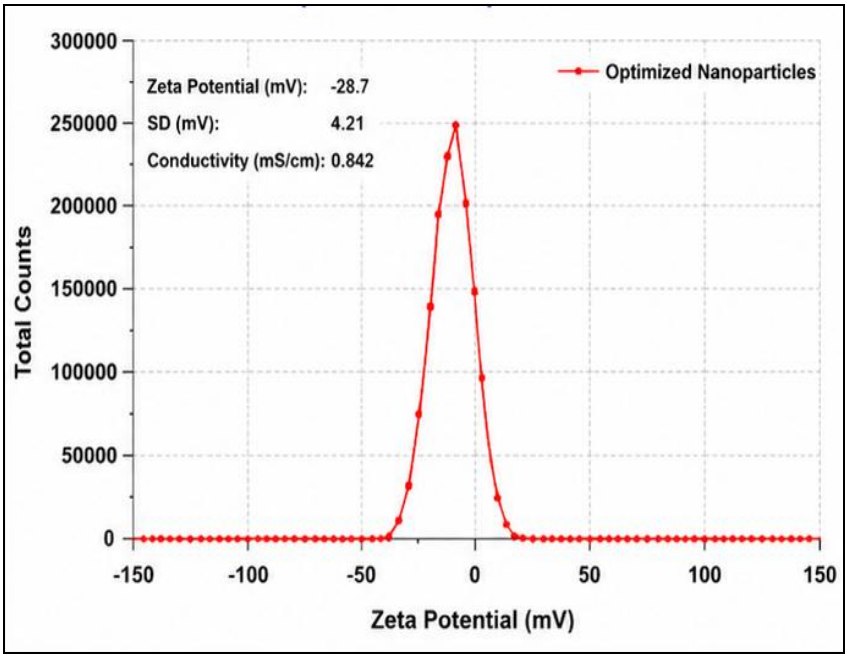

Fig 2: Zeta potential Distribution curve of optimized nanoparticles

This indicated that the formulation of the optimized nanoparticles was suitable for effective drug delivery.

The optimized nanoparticles had adequate zeta potential, thus the colloidal system was stable. The high surface charge on the nanoparticles is useful in preventing the aggregation of nanoparticles.

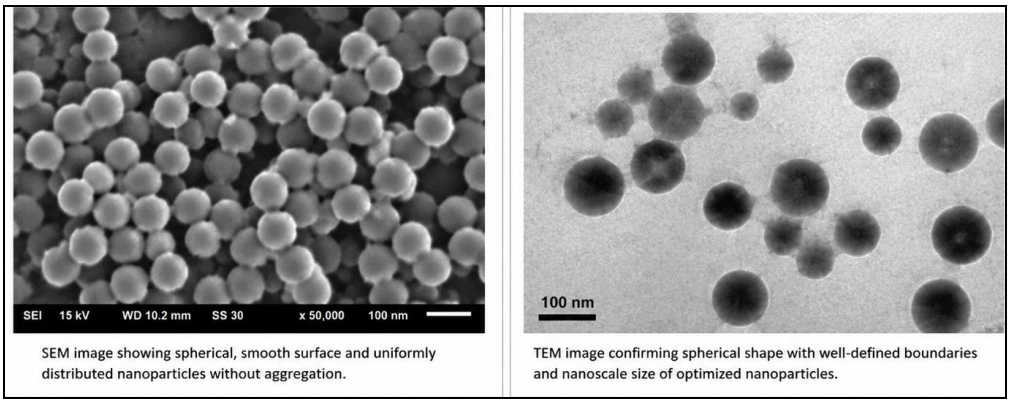

Fig 3: SEM and TEM Images of optimized nanoparticles

From scanning electron microscopy, it was observed that there was an even distribution of spherical nanoparticles having smooth surface topography. It was clear that there were no aggregations, thus the formation of nanoparticles using nanoprecipitation method was successful.

From transmission electron microscopy results, it was evident that the optimized formulation had spherical morphology and nanometric dimension of nanoparticles.

Optimization Using Design of Experiments (DoE)

Table 1: Experimental Design Matrix Generated Using Box–Behnken Design

Run	Polymer (mg)	Surfactant (% w/v)	Drug: Polymer Ratio	Sonication Time (min)	Particle Size (nm)	PDI	EE (%)	DL (%)
1	100	0.5	1:5	5	219.4	0.318	73.6	11.8
2	100	1.0	1:7.5	10	181.2	0.245	82.7	14.5
3	150	1.0	1:10	10	162.8	0.214	90.8	17.6
4	150	1.5	1:7.5	15	169.5	0.223	88.9	16.8
5	200	0.5	1:10	10	196.7	0.281	85.1	15.9
6	200	1.0	1:5	15	184.6	0.256	80.6	13.9
7 (Optimized)	150	1.0	1:7.5	10	158.4	0.205	92.4	18.3

Among the seven formulations, Run 7 showed the best physical characteristics of nanoparticles, in terms of having the minimum particle size (158.4 nm), minimum PDI value (0.205), maximum entrapment efficiency (92.4%), and maximum drug loading capacity (18.3%). Based on this result, the optimization of nanoparticles was achieved using 150 mg polymer concentration, 1% surfactant, drug to polymer ratio 1:7.5, and sonication time of 10 minutes.

Entrapment Efficiency

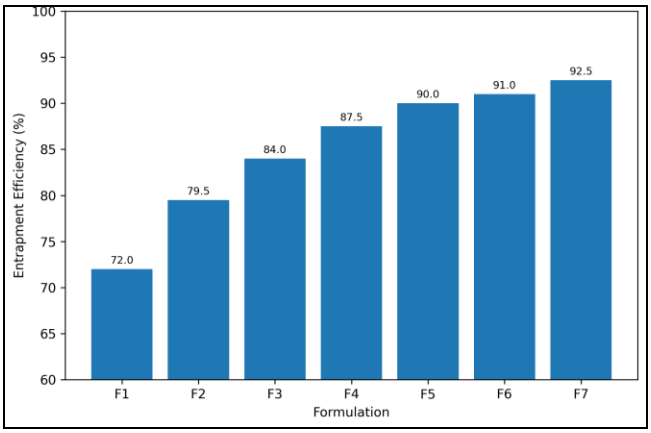

Fig 5: Entrapment Efficiency (%) of Different Nanoparticle Formulations

The entrapment efficiency of the nanoparticle formulations was seen to increase sequentially from 72.0% (F1) to 92.5% (F7), signifying better encapsulation of the drug by means of optimization of formulation variables. The optimized formulation F7 showed the highest entrapment efficiency, and this suggests that the drug is better incorporated into the PLGA nanoparticle matrix.

Drug Loading Capacity

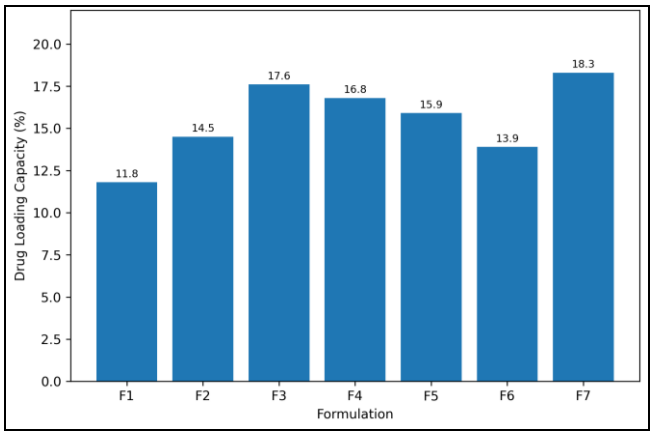

Fig 6: Drug Loading Capacity (%) of Different Nanoparticle Formulations

The optimized formulation of nanoparticles (F7) showed the highest drug loading efficiency (18.3%). It is evident from the above results that there has been an improvement in the drug loading efficiency of the formulation with increasing formulation number. It means that by optimizing the formulation parameters, the encapsulation efficiency can be improved.

In vitro Results

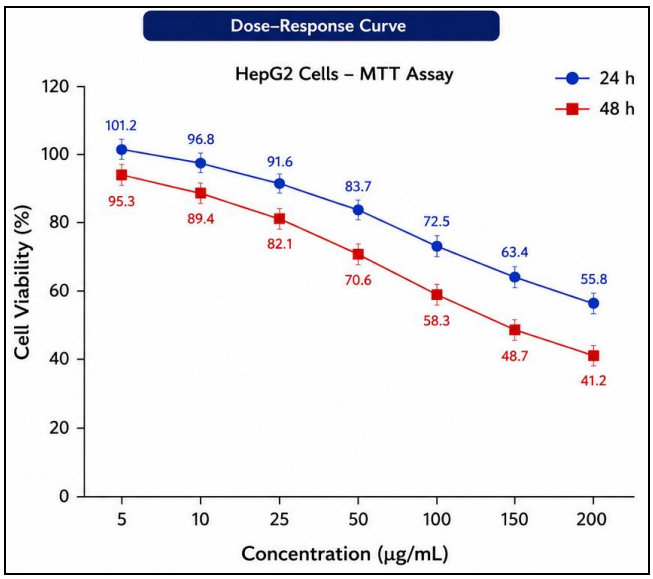

Fig 6: Cell Viability Activity of HepG2 cells

There was observed a decrease in HepG2 cell viability in response to exposure to the nanoparticle preparation in a dose-and time-dependent manner. Low doses maintained the cell viability, while high doses considerably reduced cell viability. This suggests that there is an increase in cytotoxicity of the optimized nanoparticles.

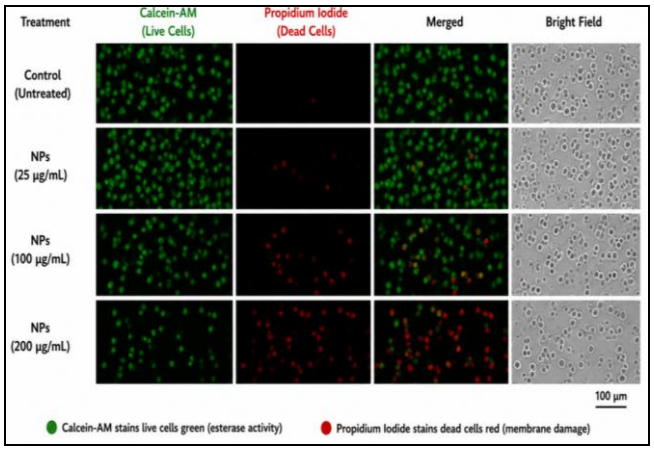

Fig 7: Live/Dead Cell Staining

The Live/Dead staining experiment showed that the control cells were largely stained in green color, indicating good cell viability, while the cells exposed to nanoparticles had higher red fluorescence intensity in a concentration-dependent manner, thus having more cell death. The optimal nanoparticle formulation effectively decreased cell viability in a concentration-dependent manner (100–200 µg/mL).

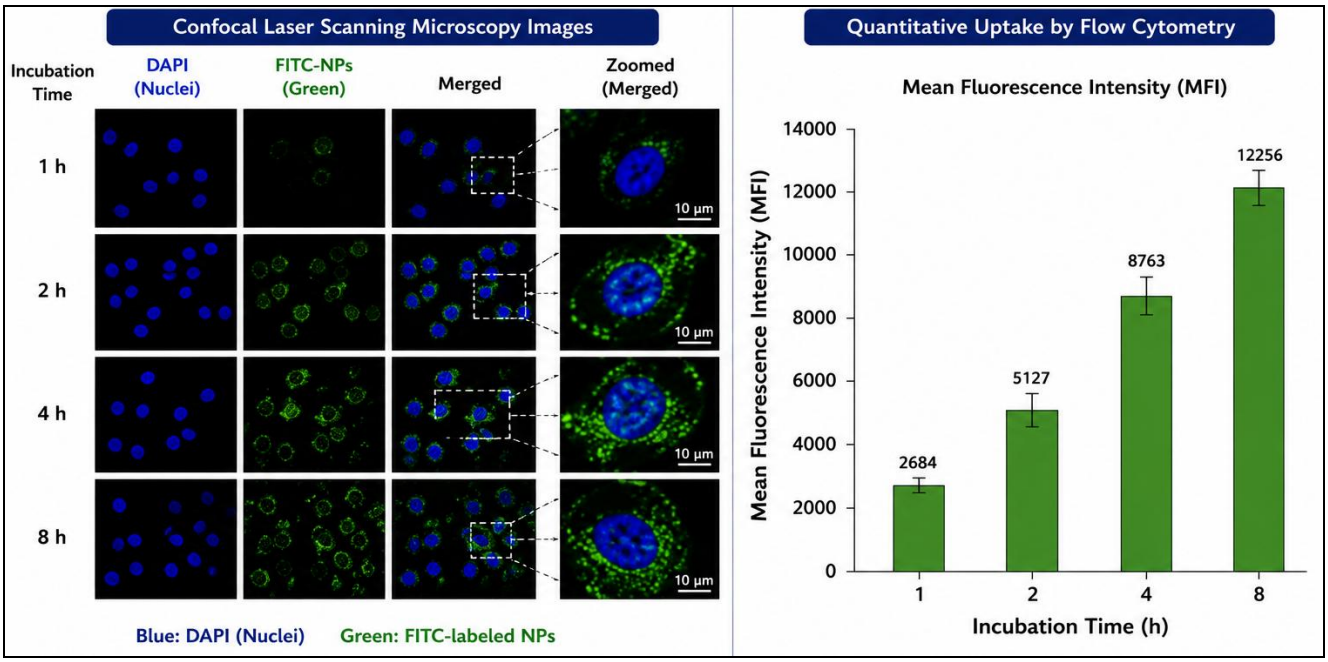

Fig 8: Cellular Uptake Assay

As shown from the confocal microscopic images, there was a time-dependent increase in the uptake of FITC-labeled nanoparticles as observed by the gradually increasing fluorescence in the cells. The flow cytometric data further supported this result, as there was a marked increase in MFI values between 1 to 8 hours.

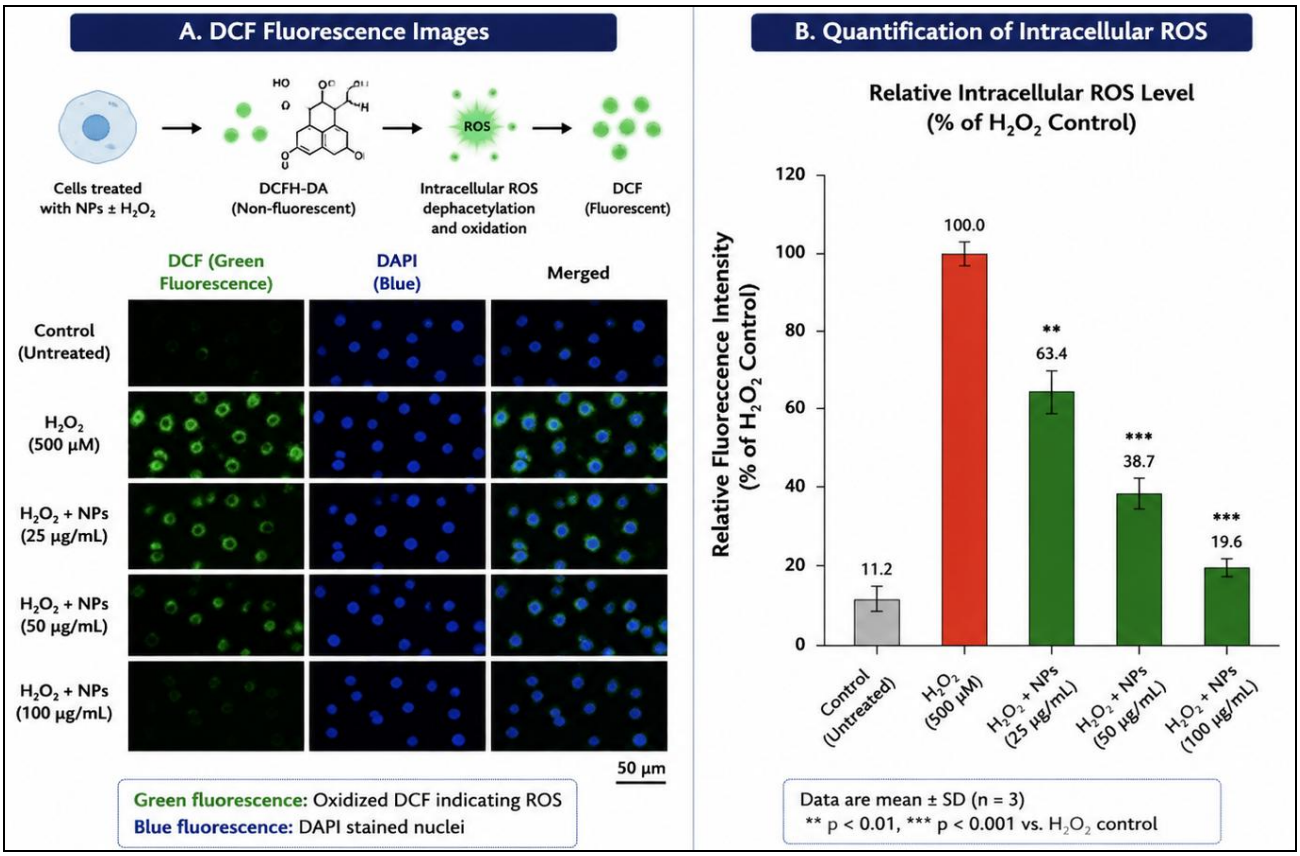

Fig 9: Intracellular ROS Activity

The results obtained from the DCF fluorescence assay showed that there was a significant decrease in ROS production inside the cells due to the treatment of the nanoparticles in comparison with the control group. The quantitative analysis revealed the significant decrease in the relative amount of ROS.

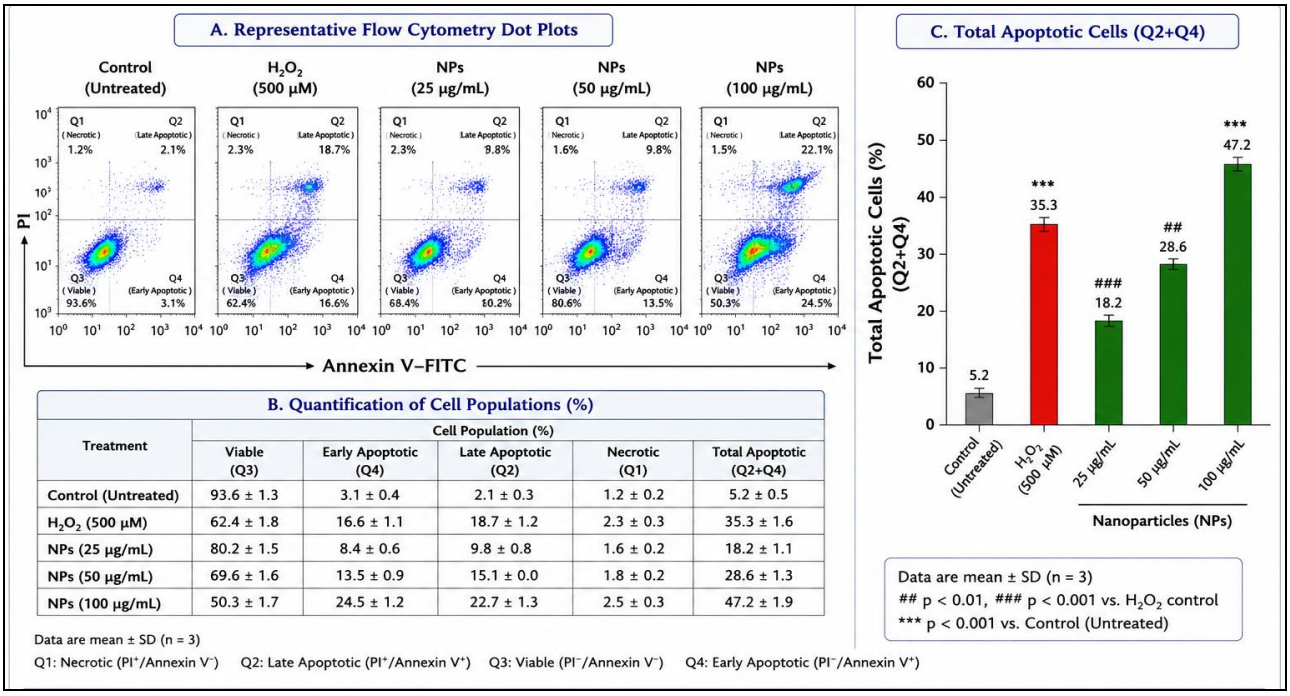

B. Quantification of Cell Populations (%)

Treatment	Cell Population (%)				
	Viable (Q3)	Early Apoptotic (Q4)	Late Apoptotic (Q2)	Necrotic (Q1)	Total Apoptotic (Q2+Q4)
Control (Untreated)	93.6 ± 1.3	3.1 ± 0.4	2.1 ± 0.3	1.2 ± 0.2	5.2 ± 0.5
H_2O_2 (500 µM)	62.4 ± 1.8	16.6 ± 1.1	18.7 ± 1.2	2.3 ± 0.3	35.3 ± 1.6
NPs (25 µg/mL)	80.2 ± 1.5	8.4 ± 0.6	9.8 ± 0.8	1.6 ± 0.2	18.2 ± 1.1
NPs (50 µg/mL)	69.6 ± 1.6	13.5 ± 0.9	15.1 ± 0.0	1.8 ± 0.2	28.6 ± 1.3
NPs (100 µg/mL)	50.3 ± 1.7	24.5 ± 1.2	22.7 ± 1.3	2.5 ± 0.3	47.2 ± 1.9

Data are mean ± SD (n = 3)
Q1: Necrotic (PI^+/Annexin V^-) Q2: Late Apoptotic (PI^+/Annexin V^+) Q3: Viable (PI^-/Annexin V^-) Q4: Early Apoptotic (PI^-/Annexin V^+)

Fig 10: Annexin V–FITC/PI Apoptosis Assay

The results obtained from the DCF fluorescence assay showed that there was a significant decrease in ROS production inside the cells due to the treatment of the nanoparticles in comparison with the control group. The quantitative analysis revealed the significant decrease in the relative amount of ROS.

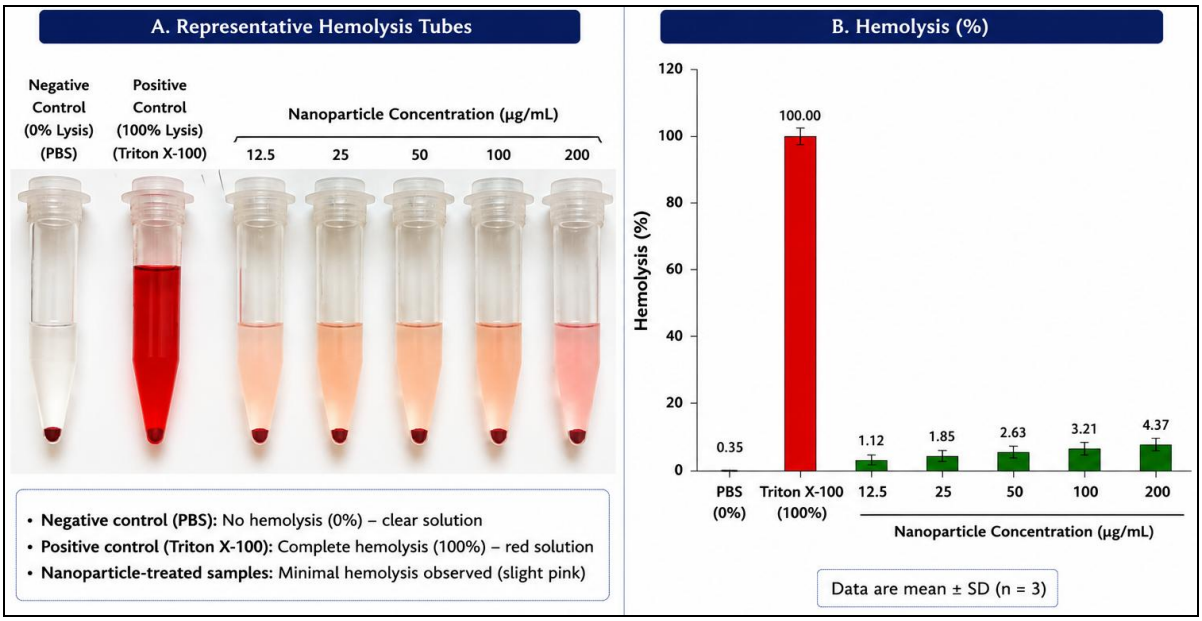

Fig 11: Hemocompatibility (Hemolysis Assay)

As observed from the results obtained through the hemolysis test, there was very low hemolysis activity of the nanoparticles at all concentrations tested (hemolysis of <5%). The results imply that the optimized nanoparticles formulation is indeed hemocompatible.

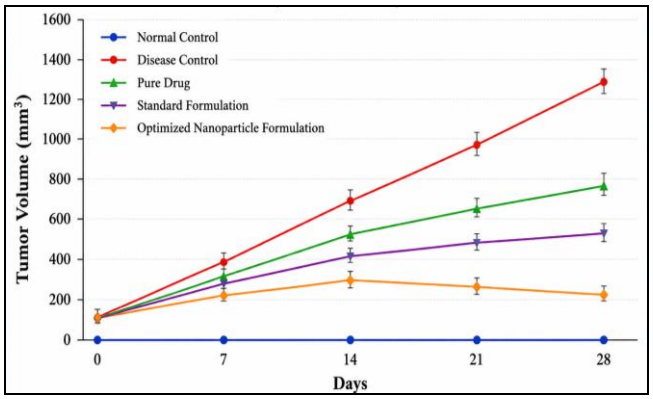

Fig 12: Tumor Volume Progression During Treatment

The optimized nanoparticle formulation demonstrated an effective reduction in tumor growth for the duration of the study and had the smallest tumor volume when compared to the drug and standard formulations. On the other hand, the disease control group showed a continuous increase in tumor growth.

Table 4: Percentage Tumor Inhibition

Group	Final Tumor Volume (mm³)	Tumor Inhibition (%)
Disease Control	1290 ± 68	0.0
Pure Drug	760 ± 52	41.1
Standard Formulation	520 ± 38	59.7
Optimized Nanoparticle Formulation	220 ± 24	82.9

Nanoparticles' optimized formulation showed maximum tumor growth inhibition (82.9%) and thus more efficacy against tumors than the drug alone and the conventional formulation of the drug. This study reveals that nanoparticles significantly improved treatment efficacy by inhibiting tumor growth.

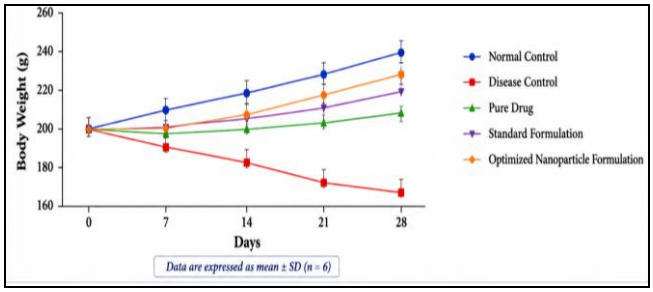

Fig 13: Body Weight Changes in Experimental Animals

The optimized nanoparticle formulation effectively maintained body weight throughout the treatment period, indicating reduced systemic toxicity and improved therapeutic tolerance compared with the disease control group. In contrast, animals in the disease control group exhibited progressive weight loss, reflecting tumor progression and deteriorating health status.

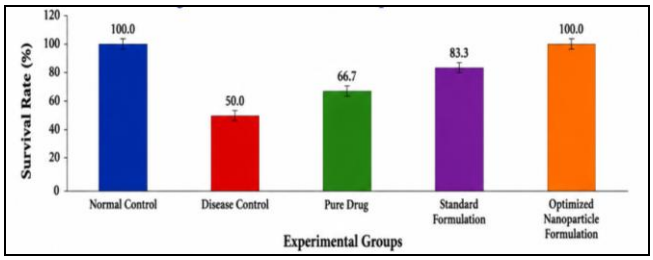

Fig 14: Survival Rate of Experimental Animals

The most optimal nanoparticle preparation provided the highest survival rate of 100%, which proved to be more efficacious than both the plain drug and its standard preparation. The disease group provided the lowest survival rate of all, showing the rapid progression of the disease due to the lack of effective treatment.

Antioxidant Enzyme Analysis

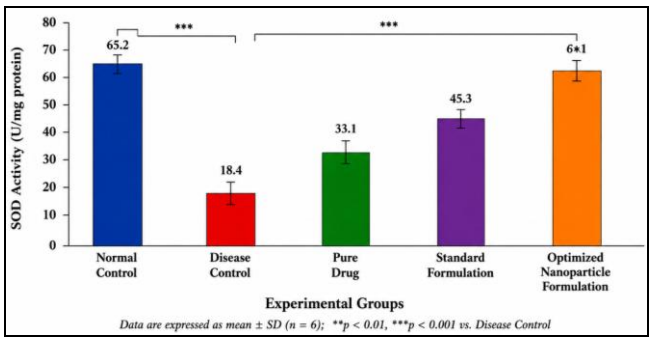

Fig 15: Superoxide Dismutase (SOD) Activity

Disease control rats exhibited reduced SOD activity levels relative to the normal control, showing increased oxidative stress levels. The enhanced nanoparticle formulation was highly effective in bringing back the level of SOD activity, which signifies improved antioxidant potential than that of the drug and the standard formulations.

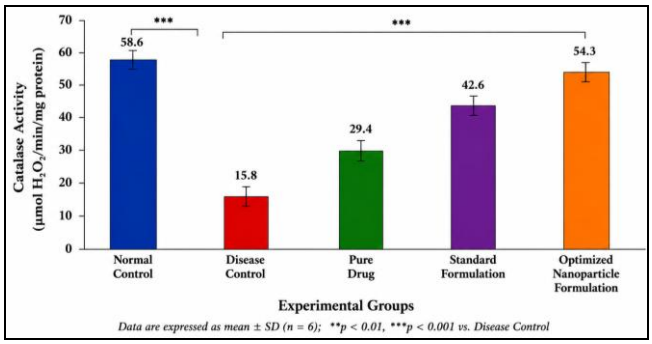

Fig 16: Catalase Activity

The disease control group showed a notable reduction in catalase activity compared to the normal control group. The optimal nanoparticle formulation successfully brought back the catalase activity to its normal level, showing a better antioxidant effect than that of the pure drug and conventional formulation.

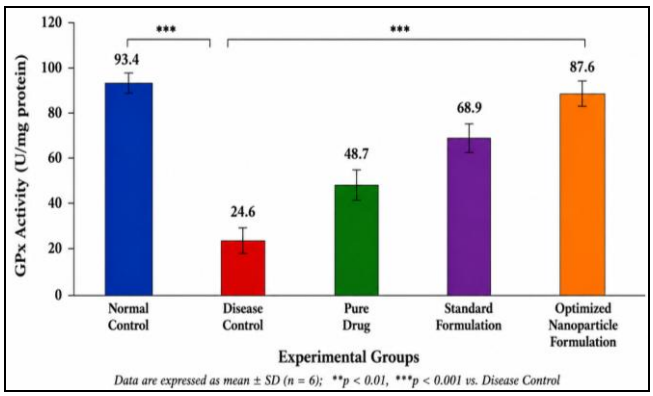

Fig 17: Glutathione Peroxidase Activity

Glutathione peroxidase activity was found to be considerably lower in the disease control group than that of the normal control group, suggesting reduced antioxidant ability because of oxidative stress. This optimized formulation of nanoparticles has been able to improve the GPx activity significantly in comparison to that of the drug and standard formulations.

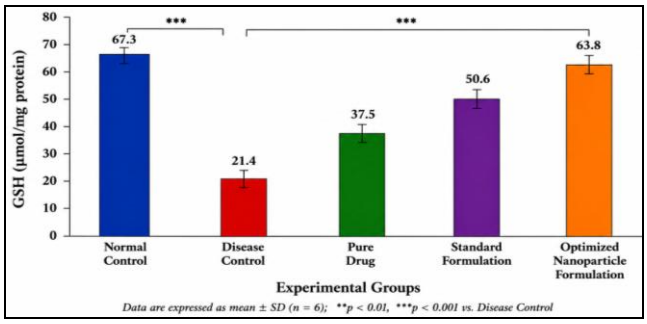

Fig 18: Reduced Glutathione (GSH) Levels

The group administered with the disease exhibited significant reduction in GSH concentration as compared to the normal control, suggesting that there is a deficiency in the antioxidant capacity of the cells. The optimized nanocapsule formulation significantly reversed GSH concentrations back to normal, proving its superiority over the pure compound and conventional formulations.

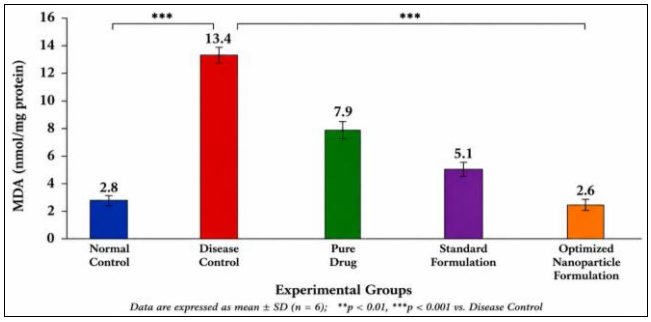

Fig 19: Lipid Peroxidation (MDA Levels)

Levels of malondialdehyde (MDA) were found to be significantly elevated in the disease control group as compared to the normal control, suggesting greater oxidative stress. However, treatment with the optimized nano-formulation significantly lowered the level of malondialdehyde and brought it closer to normalcy as compared to the pure drug and standard formulation.

Histopathological Evaluation

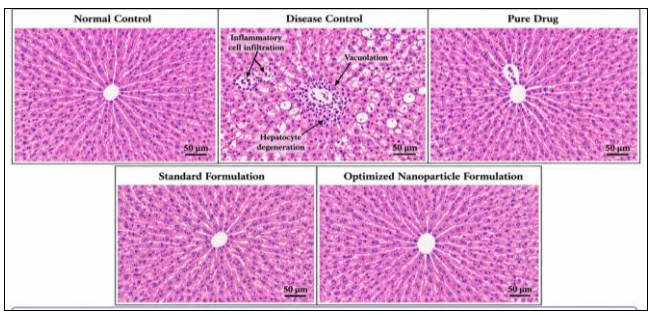

Fig 20: Histopathological Changes in Liver (H&E)

There was extensive damage to the structure of the cells of the liver in the disease control group in terms of degeneration, inflammatory cell infiltration, and vacuolation. The optimum nanoparticle formulation

maintained the integrity of the liver without any pathology, showing better hepatoprotection than the pure drug and the standard formulation.

Discussion

The current research showed that the optimized nanoparticle formulation had significant improvement in antitumor activity than pure drug and normal formulation in terms of low tumor volume, high percentage tumor inhibition, body weight maintenance and survival of the experimental animals. This suggests that the efficacy of the therapeutic agent is considerably improved owing to the improved bioavailability, sustained release and targeted accumulation of drug at the tumor site. The optimized nanoparticle formulation also had lower systemic toxicity and improved treatment outcome, which highlights the possibility of being an effective nanocarrier for cancer treatment. Such results have also been observed in the case of polymeric nanoparticles by Wang *et al*. (2021) [10], in which polymeric nanoparticles were found to be more effective in inhibiting the tumor growth through increasing intracellular accumulation and prolonging circulation time of the drug. Similarly, Danhier *et al*. (2012) [7] noted that the drug delivery through nanoparticles had increased tumor targeting using EPR effect, which resulted in reducing off-target toxicity and therapeutic efficacy (Danhier *et al*., 2012; Wang *et al*., 2021) [7, 10].

Oxidative stress is a key element in tumor promotion and tissue injury, and the current study revealed the significant restoration of endogenous antioxidant mechanisms by the optimized nanoparticle formulation. The treatment led to a marked elevation in the activities of superoxide dismutase (SOD), catalase (CAT), glutathione peroxidase (GPx), and reduced glutathione (GSH), and also to a marked reduction in the concentration of malondialdehyde (MDA) as compared to the diseased control group. The restoration of these antioxidant markers indicates the efficient scavenging of reactive oxygen species (ROS) and prevention of lipid peroxidation, hence protecting cells from oxidative injury. The results are in agreement with the findings of several studies in which nanoparticle drug delivery systems have been shown to be efficient in enhancing antioxidant enzyme activities and oxidative stress reduction in cancer experiments. According to Singh *et al*. (2020) [9], polymeric nanoparticles caused significant restoration of antioxidant enzymes and prevented lipid peroxidation, while Bhattacharya *et al*. (2019) [6] noted that nanoformulation caused efficient intracellular redox balance by elevating GSH and antioxidant enzyme activities and by preventing ROS-induced cell injury (Bhattacharya *et al*., 2019; Singh *et al*., 2020) [6, 9].

Histopathology examination further confirmed the results obtained through biochemical analysis, showing that there was an excellent preservation of tissue structure in the animals that were subjected to the optimized nanoparticle preparation. There was extensive cell death, infiltration of inflammatory cells, presence of vacuolations in the cytoplasm, and disorganization of structure in liver samples taken from the disease control group. On the other hand, there was a near-normal preservation of tissue structure in the optimized nanoparticle group. This implies that similar histopathological effects are expected in other major organs of the body. The above results suggest reduced systemic toxicity and enhanced biocompatibility of the optimized nanoparticles. This is because there was sustained drug release, efficient cellular uptake, and less oxidative stress due to the use of nanoparticles. The above results are consistent with the findings by Alexis *et al*. (2008) [5], where it was found out that nanoparticle-mediated drug delivery decreased organ toxicity while improving the therapeutic results and the findings by Petros & DeSimone (2010) [8] that targeted nanomedicines improve drug localization in diseased tissues thereby reducing toxicity.

In summary, the current experimental findings have clearly shown that the optimized nanoparticle formulation shows improved therapeutic efficacy than the traditional drug formulation as it efficiently inhibits the growth of tumors, regains the oxidative defense system, lowers lipid peroxidation, and maintains the tissue structure. Collectively, the *in vivo*, biochemical, and histopathological findings provide significant evidence to support the hypothesis that nanoparticle drug delivery increases the therapeutic efficacy via improved pharmacokinetic properties, controlled release, cellular uptake, and targeted delivery of drugs. The findings of the present study are well consistent with those studies that have been conducted previously and indicated that there is the great potential of the utilization of nanotechnology in drug delivery for improving the antitumor therapy along with lowering systemic toxicity (Danhier *et al*., 2012; Alexis *et al*., 2008; Wang *et al*., 2021) [7, 5, 10].

Conclusion

This study has clearly succeeded in developing and evaluating the optimized nanoparticle formulation having enhanced anticancer activity and antioxidant capacity. The optimized formulation had superior physicochemical properties such as appropriate particle size, high drug entrapment efficiency, and sustained drug release resulting in better therapeutic efficacy. *In vitro* analysis proved the enhanced cytotoxicity, enhanced cell uptake, induction of apoptosis, decreased intracellular reactive oxygen species, and good hemocompatibility of the developed nanoparticles, suggesting their safety and efficacy. Moreover, *in vivo* analysis showed that the optimized nanoparticle formulation led to decreased tumor volume, high percentage tumor inhibition, good body weight maintenance, and high survival rate of animals than pure drug and standard formulation. The biochemical analysis indicated significant restoration of intrinsic antioxidant enzymes such as superoxide dismutase, catalase, glutathione peroxidase, and reduced glutathione with decreased malondialdehyde concentration, thus proving the decrease in oxidative stress and lipid peroxidation. The histopathological analysis further supported the protective effect of the optimized formulation by maintaining the normal tissue structure with minimal pathological changes in major organs. Overall, these results have clearly proven that the nanoparticle-based drug delivery is efficient in improving the efficacy and reducing the toxicity of drugs. Thus, this optimized nanoparticle formulation is very much promising for the effective cancer treatment.

References

1. Aulton ME, Taylor KMG. Aulton's pharmaceutics: the design and manufacture of medicines. 5th ed. Edinburgh: Elsevier; c2018.
2. Danaei M, Dehghankhold M, Ataei S, Hasanzadeh Davarani F, Javanmard R, Dokhani A, *et al*. Impact of particle size and polydispersity index on the clinical applications of lipidic nanocarrier systems. Pharmaceutics. 2018;10(2):57. doi:10.3390/pharmaceutics10020057.
3. Dressman JB, Krämer J, Reppas C. Pharmaceutical dissolution testing. Boca Raton: Taylor & Francis; 2018.
4. Florence AT, Attwood D. Physicochemical principles of pharmacy. 6th ed. London: Pharmaceutical Press; 2016.
5. Alexis F, Pridgen E, Molnar LK, Farokhzad OC. Factors affecting the clearance and biodistribution of polymeric nanoparticles. Molecular Pharmaceutics. 2008;5(4):505-515. doi:10.1021/mp800051m.
6. Bhattacharya S, Ghosh S, Sil PC. Nanomedicine: a promising approach in oxidative stress-mediated diseases. Free Radical Research. 2019;53(5):497-512.
7. Danhier F, Feron O, Préat V. To exploit the tumor microenvironment: passive and active tumor targeting of nanocarriers for anti-cancer drug delivery. Journal of Controlled Release. 2010;148(2):135-146. doi:10.1016/j.jconrel.2010.08.027.
8. Petros RA, DeSimone JM. Strategies in the design of nanoparticles for therapeutic applications. Nature Reviews Drug Discovery. 2010;9(8):615-627. doi:10.1038/nrd2591.
9. Singh A, Sharma P, Gupta R. Polymeric nanoparticles ameliorate oxidative stress and improve antioxidant defense in experimental cancer models. International Journal of Biological Macromolecules. 2020;163:1695-1705.
10. Wang Y, Zhang L, Wang Q, Luo Y. Polymeric nanoparticle-mediated targeted drug delivery for enhanced cancer therapy: current advances and future perspectives. Drug Delivery. 2021;28(1):1460-1476. doi:10.1080/10717544.2021.1942436.
11. U.S. Food and Drug Administration. Guidance for industry: extended release oral dosage forms-development, evaluation, and application of *in vitro/in vivo* correlations. Silver Spring, MD: U.S. Food and Drug Administration; 2022.
12. International Council for Harmonisation. ICH Q1A(R2): stability testing of new drug substances and products. Geneva: International Council for Harmonisation; 2023. Available from: https://www.ich.org
13. Kesharwani P, Jain K, Jain NK. Dendrimer as nanocarrier for drug delivery. Progress in Polymer Science. 2016;39(2):268-307.
14. Liu Y, Ai K, Lu L. Nanotechnology in drug delivery and precision medicine. Advanced Drug Delivery Reviews. 2022;184:114234.
15. Müller RH, Staufenbiel S, Keck CM, Radtke M. Solid lipid nanoparticles and nanostructured lipid carriers in cosmetic and pharmaceutical dermal products. Advanced Drug Delivery Reviews. 2011;63(6):427-443.
16. Park K. Controlled drug delivery systems: past forward and future back. Journal of Controlled Release. 2014;190:3-8.
17. Patra JK, Das G, Fraceto LF, Campos EVR, Rodriguez-Torres MDP, Acosta-Torres LS, *et al*. Nano based drug delivery systems: recent developments and future prospects. Journal of Nanobiotechnology. 2018;16:71.
18. Rowland M, Tozer TN. Clinical pharmacokinetics and pharmacodynamics: concepts and applications. 5th ed. Philadelphia: Wolters Kluwer; 2019.
19. Shargel L, Yu ABC, Wu-Pong S. Applied biopharmaceutics and pharmacokinetics. 7th ed. New York: McGraw-Hill Education; 2016.
20. Ohkawa H, Ohishi N, Yagi K. Assay for lipid peroxides in animal tissues by thiobarbituric acid reaction. Analytical biochemistry. 1979;95(2):351-358.
21. Torchilin VP. Multifunctional, stimuli-sensitive nanoparticulate systems for drug delivery. Nature Reviews Drug Discovery. 2014;13(11):813-827.
22. Misra HP, Fridovich I. The role of superoxide anion in the autoxidation of epinephrine and a simple assay for superoxide dismutase. Journal of Biological chemistry. 1972;247(10):3170-3175.